

Report on the Characterization of CO₂
Absorption and Release in
1-Butyl-3-Methylimidazolum Acetate

Jacob Killelea - ASEN 4849: Independent Study

May 13, 2019

Abstract

An overview of work conducted to date is presented on the study of 1-butyl-3-methylimidazolum acetate (BMIM Ac)'s ability to reversibly adsorb carbon dioxide (CO₂) under 2 torr partial pressure (ppCO₂) equivalent conditions. This work demonstrates potential methods of removing CO₂ from BMIM Ac, as well as the challenges of creating repeatable conditions with this liquid.

Contents

1	Introduction	3
1.1	Previous Work at CU	3
2	Materials and Methods	4
2.1	Materials	4
2.2	Methods	5
2.2.1	Experimental Setup - Vacuum Desorption	5
2.2.2	Experimental Setup - Argon Sparge	5
2.2.3	Glassware Preparation	6
2.2.4	Experiment Preparation	6
2.2.5	Vacuum Drying	6
2.2.6	Argon Sparge Drying	7
2.2.7	Sorption	8
2.2.8	Vacuum Desorption	10
2.2.9	Argon Sparge Desorption	11
3	Uncertainty Analysis	12
3.1	Measurement Uncertainty	12
3.2	Derived Parameters	13
3.3	Uncertainty in Preparation and Drying	13
3.4	Uncertainty in Sorption	14
3.5	Uncertainty in Desorption	15
4	Results	17
4.1	Sorption After Vacuum Drying	17
4.2	Sorption After Argon Sparge Drying	18
4.3	Desorption with Vacuum	19
4.4	Desorption with Argon Sparge	20
5	Conclusions and Lessons Learned	20
6	Future Work	21
7	Appendix	22
7.1	January 14th	22
7.2	February 1st	24
7.3	February 9th	26
7.4	February 16th	28
7.5	March 1st	31
7.6	March 16th	33
7.7	April 6th	36
7.8	April 13th	38
7.9	April 27th	40

1 Introduction

1-Butyl-3-Methylimidazolium Acetate (BMIM Ac) is a member of a new class of chemicals called ionic liquids (ILs), which are room temperature salts where both the anion and cation are large organic molecules. ILs are stable and nontoxic over a wide range of temperatures and have a negligible vapor pressure. In addition, the large family of ILs means that many different liquids exist, with a variety of different properties. For example, similar ionic liquids include 1-butyl-3-methylimidazolium tetrafluoroborate and 1-ethyl-3-methylimidazolium acetate. In particular, BMIM Ac shows potential for use in CO₂ removal systems for future spacecraft because CO₂ dissolves readily and reversibly in it through chemical, as well as physical, action [1].

Because BMIM Ac is a liquid, it has additional advantages over the current system on the International Space Station (ISS), the Carbon Dioxide Removal Assembly (CDRA). CDRA has reliability and capability deficiencies that appear to be related to its pelletized Zeolite 5A sorbent. CDRA's sorbent beds are regenerated with a thermal-vacuum cycle during which the bed cannot be used to adsorb more CO₂. In addition, this cycle appears to create dust from the pellets. This dust increases the pressure differential across the sorbent beds and degrades the system's performance overall [1]. Finally, CDRA does not meet guidelines for future space missions. While CDRA keeps the ISS's atmosphere at roughly 4 torr ppCO₂, the National Aeronautics and Space Administration's (NASA's) Life Support Baseline Values and Assumptions document acknowledges that astronaut performance and comfort can begin to degrade as early as 2.3 to 2.7 torr ppCO₂ [2]. Consequently, NASA's new goal is for future spacecraft atmospheres to reduce ppCO₂ to 2 torr or below.

In comparison, BMIM Ac does not produce dust. Its foreseeable application is in a supported ionic liquid membrane or a direct liquid contactor design [1] [4], where operation occurs at a steady state, instead of CDRA's cycles. This improves reliability and predictability of operation.

As attention turns to the potential for ILs to replace solid sorbents, a knowledge gap has been found regarding BMIM Ac's ability to adsorb and release CO₂ at low partial pressures, such as NASA's 2 torr goal. In particular, because BMIM Ac adsorbs CO₂ using both chemical and physical action, its absorption capability exceeds Henry's law. Where 2 torr of CO₂ is 0.26% of an ideal gas mixture, BMIM Ac will adsorb up to a 1.67% weight concentration under these conditions [3].

An accurate characterization of these liquids will aid in understanding their CO₂ carrying and membrane transport characteristics.

1.1 Previous Work at CU

Here at the University of Colorado Boulder, the CARIL graduate project from the spring of 2017 examined novel carbon dioxide removal system designs with the intent of informing future ECLSS systems. They modeled and built two CO₂ removal assemblies, one with direct liquid contact channels and another

with hollow fiber membranes. In the direct liquid contact design, process gas is flown over the IL, which is pumped through open channels such that the gas and liquid have a direct contact interface. In the hollow fiber design, process gas is flown through the hollow fibers contained inside a larger pipe, while IL is pumped in the opposite direction on the outside of the fibers. The porosity of the fibers allows the IL to permeate them and make contact with the process gas in order to facilitate the removal of CO₂ [1].

In addition, Brett Shaffer, a previous student working under Professor James Nabity, investigated the production of 2 torr saturation solutions from fully saturated ones, as well as their ability to release CO₂ under elevated temperature (50 to 80 Celsius) and reduced pressure (150 to 500 millitorr). While his results showed good reversibility, he did not fully remove dissolved gasses and water from the IL beforehand and, consequently, some results showed that under reduced pressure and elevated temperature, more mass could be lost than was initially adsorbed, negating the validity of those results [3].

This series of experiments continued where Brett left off, with the addition of a pre-saturation drying step to try and remove gasses and liquids that may initially be dissolved in the IL.

2 Materials and Methods

2.1 Materials

Materials used over the course of these experiments include:

- BMIM Ac, CAS: 284049-75-8, from Sigma Aldrich, lot number BCBM4905V, with a purity of ≥ 95%.
- Argon (Ar), from Airgas. Lot and purity information unavailable.
- Carbon Dioxide (CO₂), from Airgas, Lot 54-124363786-4, 99.999% pure.
- Cole-Parmer Symmetry PA-224 analytical balance.
- CPS ProSet VP2D vacuum pump.
- Omega HH42A digital temperature gauge.
- Omega OVG64 digital vacuum gauge.
- Bante MS300 Hot Plate.
- 125 mL Pyrex side arm flask.
- Pyrex dish, 125 mm by 65 mm.
- Vulcanized rubber stopper for flask.
- 250 and 50 mL Pyrex beakers.

- 2 fritted glass bubblers from Fisher.
- 2 pipettes per run.
- 4 large Kimtech wipes (kimiwipes) per run.
- Deionized water, $17 \text{ M}\Omega/\text{cm}$.
- Isopropyl alcohol, 99%.
- Alicat Scientific MCE-100SCCM-D/5M Flow Regulator/Flow Meter.
- Alicat Whisper MW-200SCCM-D/5M Flow Meter.
- Vacuum chamber for storage, approx 2m^3 , with pumping ability down to 11-12 mTorr.
- 500 mL Pyrex beaker.
- Vulcanized rubber stopper for beaker, with holes in top.
- Approximately 1.5 meters of wire reinforced vacuum hose.
- Miscellaneous hose fittings and hose clamps.
- DuPont vacuum grease.

2.2 Methods

2.2.1 Experimental Setup - Vacuum Desorption

In these experiments, the side arm flask containing IL was connected via vacuum hose to the CPS ProSet vacuum pump through the Omega vacuum gauge and two hoses terminating in the stopper on the 500 mL flask, which acted as a liquid trap in the case of spillage or overflowing. The connection between the side arm and the hose was sealed with vacuum grease. The stopper and fittings on the stopper for the 500 mL flask were as well. The connections on the vacuum pump and vacuum gauge were sealed with hose clamps. This setup was used for both the initial drying phase and the desorption phase of each experiment. The flask was lowered into a water bath heated by a Bante hot plate. Sous vide (PVC) balls were used to cover the water in order to limit evaporation.

2.2.2 Experimental Setup - Argon Sparge

In these experiments, the side arm flask containing IL used a stopper with two holes bored through the top. One of the holes was used to position a fritted glass bubbler such that the fritted glass element sat below the liquid level of the IL. The bubbler was connected with plastic hosing to an Argon bottle through an Alicat flow meter. The flask was lowered into a water bath heated by a Bante hot plate. Sous vide (PVC) balls were used to cover the water in order to limit evaporation.

2.2.3 Glassware Preparation

The glassware, except the Pyrex tray and 500 mL beaker, was cleaned and washed between every experimental run. In cases where the side arm flask was used to store IL between runs, the IL was transferred to a 250 ml beaker. The flask was then wiped clean of remaining droplets of IL with Kimtech wipes (kimiwipes). All of the glassware was then washed in a three step process. Washes progressed from tap water, to filtered deionized water, and then isopropyl alcohol. Beakers and flasks were wiped dry with kimiwipes between each wash, while fritted glass bubblers were left to air dry between washes. The glassware was then either left to air dry, or placed in the large vacuum chamber to evaporate the remaining isopropyl alcohol.

2.2.4 Experiment Preparation

The side arm flask was retrieved from storage or the vacuum chamber and placed on a Cole-Parmer Symmetry PA 224 analytical balance and its weight recorded.

Then, the BMIM Ac was retrieved from storage or the vacuum chamber and poured into the sidearm flask, the flask placed back on the balance, and the weight again recorded.

A clean, vulcanized rubber stopper was then temporarily added to the mouth of the flask and weighed again. The stoppers used are of vulcanized rubber with two holes approximately five millimeters in diameter. For runs under reduced pressure, these holes were sealed with machine screws coated in DuPont vacuum grease. The stopper then was removed and a strip of the vacuum grease was applied around the side of the stopper before it was reinserted and weighed again, allowing for the individual weights of each component (flask, IL, stopper, and vacuum grease) to be recorded separately.

2.2.5 Vacuum Drying

In order to remove water and dissolved gasses from the IL, initial runs had the IL was heated in a water bath under vacuum for 1.5 to 47 hours. The heat was provided by a Bante hot plate with closed loop control, while a CPS Pro Set VP2D two stage vacuum pump was connected through an Omega vacuum gauge and a liquid trap to the side arm of the flask with wire reinforced plastic tubing. During the drying stage, the water bath was kept at 70 to 80 degrees Celsius, with regular fluctuations of $\pm 1^{\circ}C$, and the pressure in the side arm flask varied between approximately 300 and 550 millitorr with regular fluctuations on the order of ± 30 millitorr. The minimum pressure is slightly higher than that reported by Brett Shaffer, despite using the same vacuum pump. Suspicion is that this may be due to wear on the pump's rotary vane mechanisms, but the precise cause is unknown. At intervals of time between 30 minutes to 2 hours, the time, temperature, pressure, and combined mass of the beaker, IL, stopper and associated grease were recorded. From these measurements, mass of IL, mass lost in the measurement interval, total mass lost, and mass loss rate are also calculated. In order to reduce errors from moisture and contaminants such

as vacuum grease used to seal the joint between the flask's side arm and the vacuum tubing, the flask's exterior was wiped dry with kimiwipes, while the side arm was wiped clean of vacuum grease, then wiped a second time with 99% isopropyl alcohol, and then wiped dry. Mass loss rate was used as an indicator of the progression of the drying of the IL. It was observed found that the loss rate reached an approximately constant value of 0.03 wt.% per hour within two hours of drying beginning. This was unexpected. Intuition suggests that mass loss rate should trend to zero over time, as in a first order decay. Without visible first order effects, judging the appropriate time to dry the IL became difficult and the duration of this phase was inconsistent over the course of the experiments. The IL was then stored in the side arm flask with stopper inserted, either with the side arm sealed with Parafilm or under reduced pressure in the large vacuum chamber.

2.2.6 Argon Sparge Drying

Based on data shared by Reaction Systems LLC in similar experiments, experiments in removing water and dissolved gasses by sparging argon through the IL was attempted. Argon is not known to be soluble in BMIM Ac, which made it an ideal gas choice for this use. In this process, the normal airtight stopper was replaced with one with two holes in it, and through one hole a fritted glass bubbler was inserted. The side arm flask was then attached through a regulator and flow meter to a bottle of argon and the gas was bubbled through the IL at approximately 95 scc/min . Periodic mass, temperature, and flow rate measurements were taken and IL mass, mass lost in the interval and overall, and mass loss rate were calculated as before. However, in some of the tests of this method, the liquid was seen to trap a large quantity of bubbles due to its viscosity at room temperature, and is shown in figure 1. This was rectified in a later test by using a hot water bath, held at 65 to 75 Celsius, which reduced viscosity and bubble loading considerably.



(a) Argon bubble loading in BMIM Ac (b) The same liquid after approximately 10 minutes in a vacuum chamber

Figure 1: Bubble loading and subsequent removal, March 16th

2.2.7 Sorption

In order to produce a 2 torr, or 1.67 wt.% equivalent solution of CO₂, a fraction of the IL was fully saturated and then mixed back into the remainder. For sorption, a 100 mL beaker was weighed, a fritted glass bubbler then was added and it was weighed again. A pre-calculated amount of IL was then added to the beaker and CO₂ was flowed through the bubbler and the IL. Initial trials did not monitor the flow rate of CO₂ into the IL. Rather, the pressure regulator on the CO₂ tank was set at 17 *psi*, which is estimated to have given a flow rate close to 100 *scc/min*. Later trials used an Alicat flow regulator, set at 95 *scc/min*, as high as the regulator would go. At regular intervals, the bubbler was disconnected from the gas flow and the beaker, bubbler, and IL were weighed on the analytical balance such that the current CO₂ concentration could be calculated.

In order to calculate the amount of IL to saturate, a target mass of 2 torr equivalent saturation was chosen, such that there was a slight excess of the dried IL available. The equivalent amount of CO₂ to adsorb at the 1 atmosphere CO₂ saturation point of 7.45 wt.% then inferred the amount of IL to saturate according to:

$$m_{CO_2} = m_{2T}\omega_{2T} \quad (1)$$

$$m_{IL,sat} = m_{CO2} \frac{1 - \omega_{100\%}}{\omega_{100\%}} \quad (2)$$

Where $\omega_{100\%}$ is the published maximum amount of CO₂ that the IL can hold, 7.45% wt.%. This amount, plus an excess of a few grams to account for residue, was added to the beaker and saturated with CO₂. The beaker was periodically taken off of the CO₂ flow to be measured. An increase in the viscosity of the IL was observed during bubbling, but this may have been because the liquid was at room temperature for this step instead of being in a hot water bath, rather than because of the addition of CO₂. Regardless, the increase in viscosity led to a tendency for small bubbles of CO₂ to be trapped, which would affect the mass measurement. Therefore, the liquid was stirred using the bubbler for 10 to 20 seconds before the beaker, bubbler, and CO₂ were weighed. From the total mass, the mass of IL was calculated, as well as the mass increase over the measurement interval, the total mass increase, and the rate of mass increase. Assuming that all the mass increase is accounted for by CO₂ the percentage CO₂ in the IL could then be calculated as:

$$\omega_{CO2} = 100\% \times \frac{m_1 - m_0}{m_0} \quad (3)$$

Where m_1 is the mass of the IL after sorption, and m_0 is the mass before. Sorption was stopped when the IL is deemed to be sufficiently close to the 7.45% saturation point [1], the published saturation limit of BMIM Ac under 1 atmosphere of 100% CO₂. However, as seen in figure 4, some trials never reached this point. A calculated mass of the saturated IL was added back to the side arm flask of dry IL such that:

$$m_{add} = \frac{m_{dry}}{(\omega/\omega_{2T}) - 1} \quad (4)$$

This calculation was used as a guideline and afterwards, the exact amount of IL added was calculated from the increase in mass and the CO₂ concentration of the new solution was calculated as:

$$\omega_{CO2} = 100\% \times \frac{m_{CO2}}{m_{IL}} \quad (5)$$

Where:

$$m_{CO2} = \omega m_{add} \quad (6)$$

$$m_{IL} = m_{dry} + m_{add} \quad (7)$$

and ω is current concentration of CO₂ in the IL being saturated.

The side arm flask would then be placed on the scale and tared, and an amount of the saturated IL was then added using a pipette. This amount was usually very close to m_{add} , with an excess of between 0.1 and 0.3 grams.

2.2.8 Vacuum Desorption

The process of desorption took place in the same manner as the initial drying of the IL. The side arm flask was placed in a hot water bath. Vacuum was applied with the same vacuum pump configuration as before, and pressure, temperature, and total mass were recorded at regular intervals using the same procedure as during the vacuum drying phase. During the first hour of drying, the IL was observed to bubble vigorously. This is assumed to be CO₂ rapidly coming out of the liquid. This is shown in Figure 2.

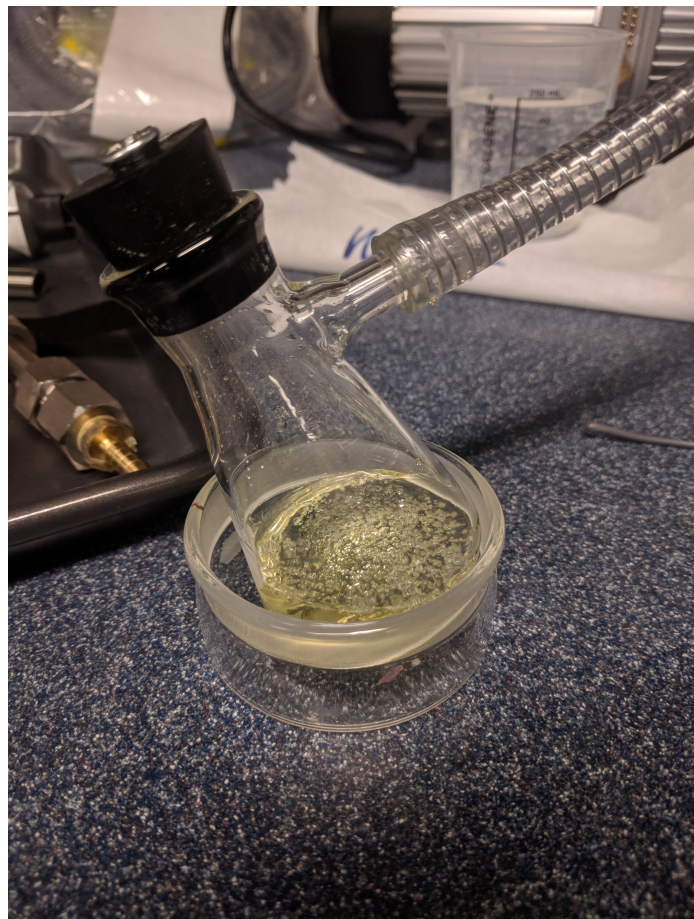


Figure 2: The side arm flask, removed from the hot water bath, showing bubble formation in the IL

Unlike the drying step, the desorption process was kept running for as long as possible. The limiting factor became time, as the CO₂ saturated liquid could not be stored without risking the CO₂ naturally desorbing, as well as the absorption

of other gasses and water. Most tests concluded after removing less than half of the CO₂ that was calculated to have been added, and running the experiments overnight unmonitored on a hot plate was seen as an unacceptable risk after a switching element in one hot plate failed short and caused the hot plate to overheat and destroy the experiment in progress. .

2.2.9 Argon Sparge Desorption

Drying with Argon as a sparge gas took place in the same manner as the drying phase, with the side arm flask immersed in a hot water bath and argon flowing through the bubbler and IL. The flow rate was monitored with an Alicat flow monitor and the temperature of the water bath was measured with an Omega temperature sensor. At regular intervals, the Argon flow rate and water bath temperature were recorded. The bubbler was then disconnected from the Argon flow and the flask removed from the hot water bath. It was then wiped dry and weighed on the analytical balance before being returned to the water bath and the Argon reconnected.

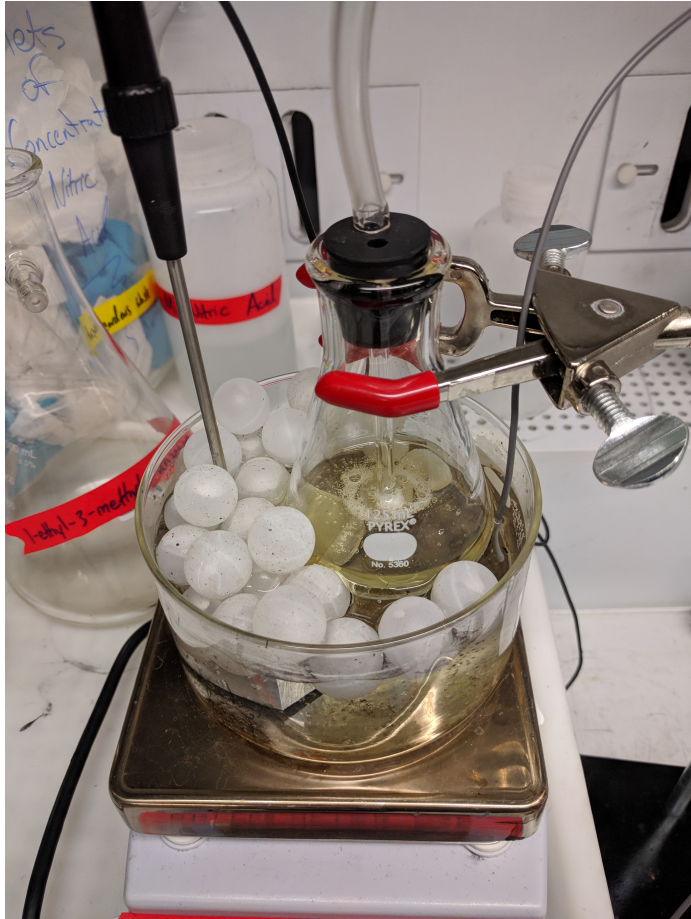


Figure 3: The setup for desorption using an Argon sparge. Pictured are the flask, hot water bath, sous vide balls, hot plate, and temperature probe.

3 Uncertainty Analysis

No direct measurement is perfect, and these uncertainties propagate through all the calculations. A thorough understanding of the uncertainty in the recorded data is needed in order to fully understand the results of the experiments.

3.1 Measurement Uncertainty

For N direct measurements of a mass, the uncertainty in the measured value x is:

$$\delta x = \frac{t}{\sqrt{N}} \sqrt{\sum_i (\delta S_i)^2} + \sqrt{\sum_j (\delta B_j)^2} \quad (8)$$

Where δS_i is the i th measurement's precision, and δB_j is the j th source of bias error, and t is from the Student t table for a given number of data points and a confidence interval. The Cole-Parmer Symmetry PA-224 specifies that a measurement is repeatable to 0.2 mg and the scale's overall linearity is 0.2 mg, so $\delta S = \delta B = 0.2$ mg. Some measurements were repeated more than once. The parameter t changes depending on the sample size, and the following table 1 was used to give a 95% confidence interval for an uncertainty of δ_{direct} .

N	t	δ_{direct} (g)
1	6.314	0.00146
2	2.920	0.00061
3	2.353	0.00047
4	2.132	0.00041
5	2.015	0.00038
6	1.943	0.00035

Table 1: t values and mass measurement uncertainties for different numbers of samples, N

3.2 Derived Parameters

Measurements which are not directly from an instrument, such as concentrations, depend on the uncertainties in the underlying physical measurements and preceding derived measurements according to:

$$U_Z = \sqrt{\sum_x \left(\frac{\partial Z}{\partial x} \delta x \right)^2} \quad (9)$$

Where the derived parameter, Z , is a function of the parameters $x_1, x_2, x_3\dots$

3.3 Uncertainty in Preparation and Drying

The first item measured is the empty side arm flask, whose mass $m = m_{flask}$, which is a direct measurement, so $\delta_{flask} = \delta_{direct}$.

After the IL is added, $m = m_{flask} + m_{IL}$, with $\delta = \delta_{direct}$. Therefore, $m_{IL} = m - m_{flask}$ and:

$$\delta m_{IL} = \sqrt{\left(\frac{\partial m_{IL}}{\partial m} \delta m \right)^2 + \left(\frac{\partial m_{IL}}{\partial m_{flask}} \delta m_{flask} \right)^2} \quad (10)$$

where

$$\frac{\partial m_{IL}}{\partial m} = 1 \quad (11)$$

and

$$\frac{\partial m_{IL}}{\partial m_{flask}} = -1 \quad (12)$$

After the stopper is added, $m = m_{flask} + m_{IL} + m_{stopper}$, so the stopper's mass is $m_{stopper} = m - m_{flask} - m_{IL}$, and the uncertainty is:

$$\delta m_{stopper} = \sqrt{\left(\frac{\partial m_{stopper}}{\partial m} \delta m\right)^2 + \left(\frac{\partial m_{stopper}}{\partial m_{flask}} \delta m_{flask}\right)^2 + \left(\frac{\partial m_{stopper}}{\partial m_{IL}} \delta m_{IL}\right)^2} \quad (13)$$

where

$$\frac{\partial m_{stopper}}{\partial m} = 1 \quad (14)$$

and

$$\frac{\partial m_{stopper}}{\partial m_{flask}} = -1 \quad (15)$$

and

$$\frac{\partial m_{stopper}}{\partial m_{IL}} = -1 \quad (16)$$

The same pattern holds for the vacuum grease measurement, where $m = m_{flask} + m_{IL} + m_{stopper} + m_{grease}$.

Each time the IL is then weighed, the parameter being measured is m , and $m_{IL} = m - m_{flask} - m_{stopper} - m_{grease}$ and the uncertainty is:

$$\delta m_{IL} = \sqrt{\left(\frac{\partial m_{IL}}{\partial m} \delta m\right)^2 + \left(\frac{\partial m_{IL}}{\partial m_{flask}} \delta m_{flask}\right)^2 + \left(\frac{\partial m_{IL}}{\partial m_{stopper}} \delta m_{stopper}\right)^2 + \left(\frac{\partial m_{IL}}{\partial m_{grease}} \delta m_{grease}\right)^2} \quad (17)$$

3.4 Uncertainty in Sorbtion

In the sorbtion step, a new clean beaker, along with a fritted glass bubbler, are used. The beaker is weighed first, with $m = m_{beaker}$ and $\delta m_{beaker} = \delta_{direct}$. Then, the scale is tared with the beaker on it and the bubbler is added such that $m = m_{bubbler}$. It is not clear what effect this has on uncertainty, but it is assumed that this is equivalent to a direct measurement such that $\delta m_{bubbler} = \delta_{direct}$. However, this is not proven and is only an assumption. Further work is needed to clarify this matter. A review of the data discovered an inconsistency in the next step. In some instances, the scale was tared with the beaker and bubbler on it such that the reading on the scale was the mass of IL added, while in others, the scale was tared with nothing on it and the mass of IL was calculated by subtracting the weight of the glassware (beaker and bubbler) from the reading on the scale. In the first case, $m = m_{IL,0}$ and $\delta m_{IL,0}$ is assumed to be δ_{direct} . In the second, $m = m_{IL,0} + m_{beaker} + m_{bubbler}$, so $m_{IL,0} = m - m_{beaker} - m_{bubbler}$. Therefore, the uncertainty in $m_{IL,0}$ is:

$$\delta m_{IL,0} = \sqrt{\left(\frac{\partial m_{IL,0}}{\partial m}\delta m\right)^2 + \left(\frac{\partial m_{IL,0}}{\partial m_{beaker}}\delta m_{beaker}\right)^2 + \left(\frac{\partial m_{IL,0}}{\partial m_{bubbler}}\delta m_{bubbler}\right)^2} \quad (18)$$

where

$$\frac{\partial m_{IL,0}}{\partial m} = 1 \quad (19)$$

and

$$\frac{\partial m_{IL,0}}{\partial m_{beaker}} = -1 \quad (20)$$

and

$$\frac{\partial m_{IL,0}}{\partial m_{bubbler}} = -1 \quad (21)$$

CO_2 is then bubbled through and adsorb into the IL, and the CO_2 concentration is calculated as in equation 5, where $m_0 = m_{IL,0}$ and $m_{CO2} = m_{IL} - m_{IL,0}$, where m_{IL} is the mass of sorbed IL at a given concentration.

The uncertainty in concentration is then:

$$\delta\omega = 100\% \times \sqrt{\left(\frac{\partial\omega}{\partial m_{CO2}}\delta m_{CO2}\right)^2 + \left(\frac{\partial\omega}{\partial m_{IL}}\delta m_{IL}\right)^2} \quad (22)$$

Where

$$\frac{\partial\omega}{\partial m_{CO2}} = \frac{1}{m_{IL}}\delta m_{CO2} \quad (23)$$

and

$$\frac{\partial\omega}{\partial m_{IL}} = -\frac{m_{CO2}}{(m_{IL})^2}\delta m_{IL} \quad (24)$$

3.5 Uncertainty in Desorption

Once the IL has been deemed to have reached an appropriate level of saturation, an amount is measured out and added back into the side arm flask of dry IL according to equation 4. The scale was tared with the side arm flask of dry IL on it, so the amount of IL added back is assumed to be a direct measurement with $\delta m_{add} = \delta_{direct}$. And the amount of CO_2 in the IL is then $m_{CO2} = \omega_{add}m_{add}$. The uncertainty of the amount of CO_2 added is:

$$\delta m_{CO2} = \sqrt{\left(\frac{\partial m_{CO2}}{\partial m_{add}}\delta m_{add}\right)^2 + \left(\frac{\partial m_{CO2}}{\partial\omega_{CO2}}\delta\omega_{CO2}\right)^2} \quad (25)$$

Where

$$\frac{\partial m_{CO2}}{\partial m_{add}} = \omega_{CO2}\delta m_{add} \quad (26)$$

and

$$\frac{\partial m_{CO2}}{\partial\omega_{CO2}} = m_{add}\delta\omega_{CO2} \quad (27)$$

The side arm flask was then taken off the scale, the stopper added back to the neck of the flask, and weighed again so that:

$$m = m_{flask} + m_{IL} + m_{stopper} + m_{grease} + m_{CO2} \quad (28)$$

Where $m_{IL} + m_{CO2} = m_{IL,sorbed}$. The amount of IL and CO₂ in the side arm flask is then:

$$m_{IL,sorbed} = m - m_{flask} - m_{stopper} - m_{grease} \quad (29)$$

The amount of IL, minus CO₂, is $m_{IL} = m_{IL,sorbed} - m_{CO2}$. And the uncertainty is:

$$\delta m_{IL} = \sqrt{\left(\frac{\partial m_{IL}}{\partial m_{IL,sorbed}}\delta m_{IL,sorbed}\right)^2 + \left(\frac{\partial m_{IL}}{\partial m_{CO2}}\delta m_{CO2}\right)^2} \quad (30)$$

Where

$$\frac{\partial m_{IL}}{\partial m_{IL,sorbed}} = \delta m_{IL,sorbed} \quad (31)$$

and

$$\frac{\partial m_{IL}}{\partial m_{CO2}} = -\delta m_{CO2} \quad (32)$$

Then, the side arm flask is placed in a hot water bath and pumped down in pressure using the vacuum pump. At each measurement interval, the mass of IL and CO₂ in the flask is:

$$m_{IL,sorbed} = m - m_{glassware} \quad (33)$$

Where $m_{glassware}$ is the mass of the flask, stopper, and vacuum grease around the stopper.

With uncertainty:

$$\delta m_{IL,sorbed} = \sqrt{\left(\frac{\partial m_{IL,sorbed}}{\partial m}\delta m\right)^2 + \left(\frac{\partial m_{IL,sorbed}}{\partial m_{glassware}}\delta m_{glassware}\right)^2} \quad (34)$$

The remaining concentration of CO₂ in the IL is then:

$$\omega_{CO2} = \frac{m_{IL,sorbed} - m_{IL}}{m_{IL}} \quad (35)$$

The uncertainty of this concentration is:

$$\delta\omega_{CO2} = \sqrt{\left(\frac{\partial\omega_{CO2}}{\partial m_{IL,sorbed}}\delta m_{IL,sorbed}\right)^2 + \left(\frac{\partial\omega_{CO2}}{\partial m_{IL}}\delta m_{IL}\right)^2} \quad (36)$$

Where

$$\frac{\partial\omega_{CO2}}{\partial m_{IL,sorbed}} = \left(\frac{1}{m_{IL,sorbed}} - \frac{m_{IL,sorbed} - m_{IL}}{(m_{IL,sorbed})^2}\right)\delta m_{IL,sorbed} \quad (37)$$

and

$$\frac{\partial\omega_{CO2}}{\partial m_{IL}} = \frac{-1}{m_{IL,sorbed}}\delta m_{IL} \quad (38)$$

4 Results

4.1 Sorption After Vacuum Drying

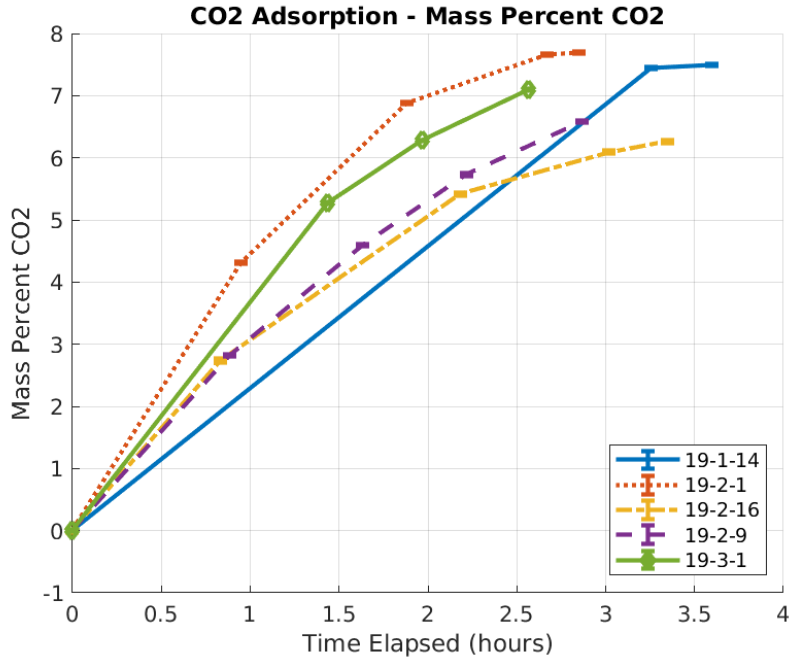


Figure 4: CO₂ uptake to saturation, trials dried with vacuum.

CO₂ Sorption in the IL appeared to follow a first order model, with the rate of update decreasing as the liquid approached saturation. However, repeatability suffered for reasons that are unclear. The actual final saturated concentration of CO₂ varied by 1.5 percent, but this comparison may not be complete as some trials, such as March 1st (data in 7.5), do not appear to have reached complete saturation. This variability in final concentration may indicate that the drying process is not being controlled well enough and some of the trials may still have residual dissolved gasses or water that is replaced by CO₂ during the sorption process, leading to no net mass increase.

The time to reach 6 percent concentration by mass - the last round number that every trial passed - varied by 1.5 hours as well, for reasons that are unclear. This change in sorption rate does not appear to be correlated to the time spent drying.

4.2 Sorption After Argon Sparge Drying

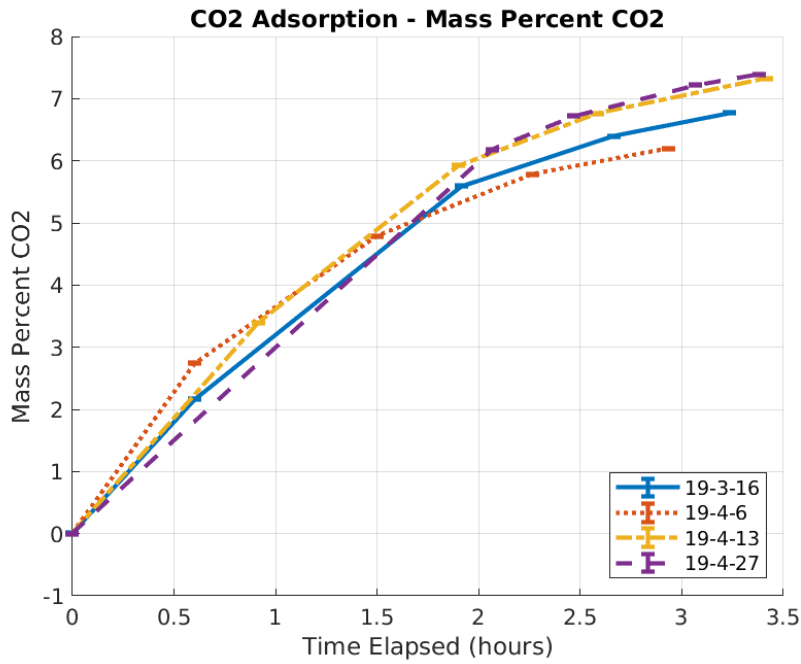
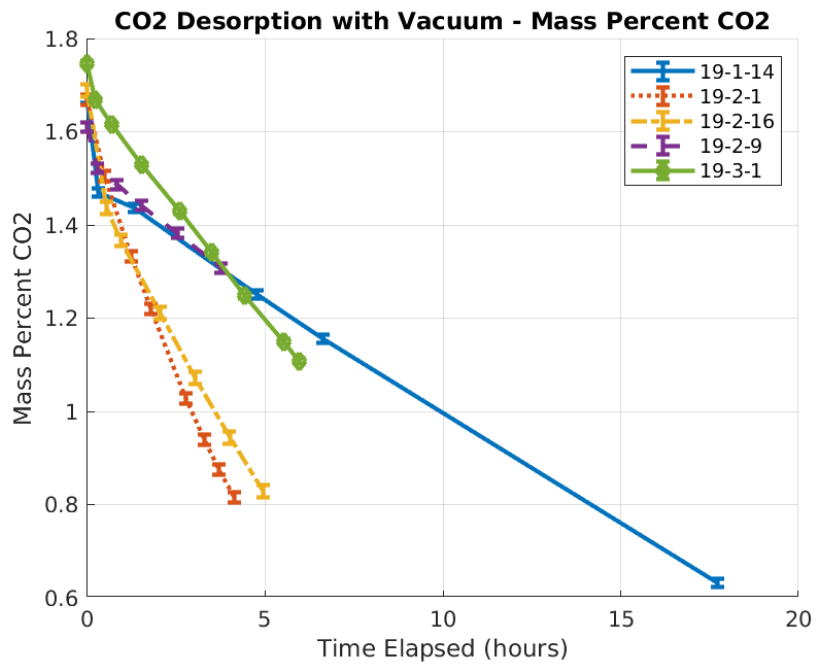


Figure 5: CO₂ uptake to saturation, trials dried with Ar sparge.

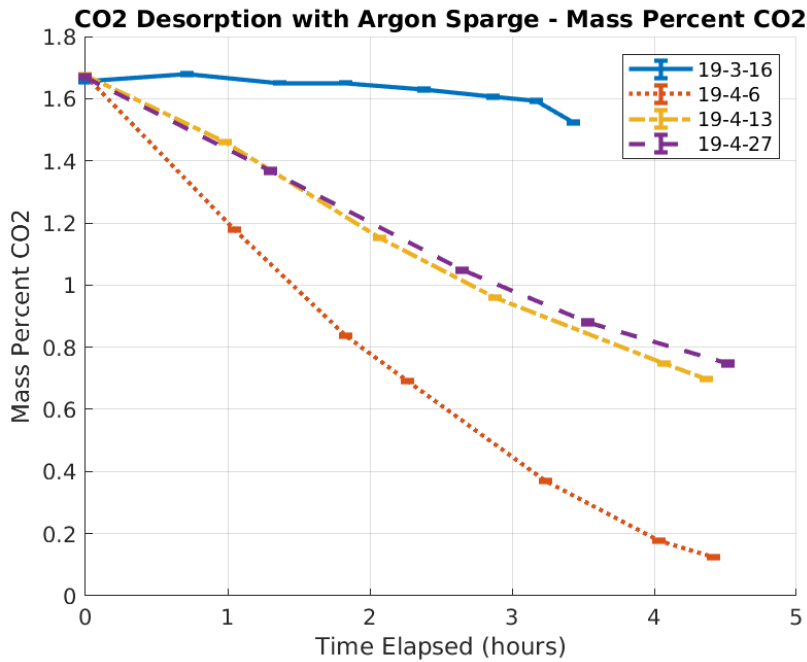
In comparison to trials using the vacuum drying method, those which used an Ar sparge show better consistency in both time to adsorb, as well as the final saturation point. However, the saturation point appears to still vary by 1 percent, which might still be attributed to variations in the drying process. In addition, the time to reach 6 percent concentration by mass still varied by 0.5 hours. Trials from April 13th and 27th (7.8 7.9), where more attention was paid to the duration of drying, show close agreement in the final concentration and the time to reach 6 percent concentration by mass, with the final concentrations varying by 0.07 percent.

4.3 Desorption with Vacuum



Desorption with vacuum shows large degrees of variability, with only February 1st (7.2) and February 16th (7.4) appearing to show desorption rate slowing down. However, the two lines appear to begin to diverge, and the 16th desorbing more slowly. The 16th's trial was dried for less time and reached a saturated CO₂ concentration 1.5 percent lower than that of the 1st's. This is different behavior than noted below, when comparing trials from April 6th and April 13th and 27th. In addition, many of these trials appear to show a sharp initial drop in mass. During the beginning of each desorption trial, the liquid would bubble vigorously as gas came out of solution and this is suspected to be the cause. It is likely that this is the gas that is physically suspended in the IL, in comparison to the CO₂ that is chemically adsorbed.

4.4 Desorption with Argon Sparge



Argon sparging shows a good potential for repeatability, particularly as demonstrated with data from April 13th and 27th (data in 7.8 and 7.9). Both were dried for 6.3 hours at 75°C. In comparison, April 6th (7.7) had a lower temperature during desorption, but was only dried for 4.4 hours at 66°C. March 16th's data (7.6) was conducted at 19°C - room temperature - and indicates that elevated temperature is necessary to avoid bubble loading and produce coherent data with this method.

5 Conclusions and Lessons Learned

This series of experiments demonstrated methods for producing solutions of CO₂ in BMIM Ac equivalent to the saturation point under 2 Torr ppCO₂, as well as the feasibility of removing said CO₂ with two different methods. However, the initial goal of reproducing Brett Shaffer's work and determining the influence of water was not accomplished. The principal reasoning is that this author did not feel comfortable leaving a hot plate running for the duration of time necessary to reach a fully desaturated state.

The most salient point uncovered is the difficulty in reproducibility between trials. The final desorption rate has numerous confounding factors, of which the most important appear to be the temperature and duration over which the

drying occurs. In general, trials where more time was spent drying the IL appear to desorb more slowly. The reason for this is still unclear. In addition, anxieties about leaving a hot plate unattended could be assuaged by using a hot plate that is designed robustly. The Bante hot plate used in this experiment only has one switching component between its power source and the heating element, and this component can easily fail, causing uncontrolled heating.

6 Future Work

Future work should first focus on establishing and verifying repeatability in the drying, sorption, and desorption processes and procedures in order to improve the comparability of different trials. After this has been established, a thorough understanding of the impact that drying duration and temperature have on the final saturation point and the desorption rate should be gained by exploring this parameter space. Finally, an attempt to repeat Brett's experiment should be made once these other factors are well understood.

7 Appendix

7.1 January 14th

Time Elapsed (hr)	Mass IL (g)	Pressure (mTorr)	Water Bath Temp ($^{\circ}C$)
0.00	58.5965	520	23
5.17	58.3089	530	70
9.28	58.1730	570	69
20.12	57.8897	560	70
23.10	57.8197	530	70
27.51	57.7330	500	71
46.97	57.4059	480	71

Table 2: Drying data from January 14th

Time Elapsed (hr)	Mass IL (g)	CO ₂ Conc (wt. percent)
0.00	17.4035 \pm 0.0029	0.0000 \pm 0.0206
3.25	18.8023 \pm 0.0029	7.4395 \pm 0.0191
3.59	18.8129 \pm 0.0029	7.4917 \pm 0.0191

Table 3: Sorption data from January 14th

Time Elapsed (hours)	IL Mass (g)	CO ₂ Conc (wt. percent)
0.00	51.2402 \pm 0.0029	1.6716 \pm 0.0090
0.31	51.1353 \pm 0.0029	1.4699 \pm 0.0090
1.33	51.1176 \pm 0.0029	1.4358 \pm 0.0090
4.76	51.0217 \pm 0.0029	1.2505 \pm 0.0090
6.62	50.9725 \pm 0.0029	1.1552 \pm 0.0090
17.72	50.7041 \pm 0.0029	0.6320 \pm 0.0091

Table 4: Desorption data from January 14th

Time Elapsed (hours)	Pressure (mTorr)	Water Bath Temp ($^{\circ}C$)
0.00	—	70
0.31	610	69
1.33	510	71
4.76	500	69
6.62	495	69
17.72	485	69

Table 5: Pressures and Temperatures during desorption, from January 14th. The missing data point at $t = 0$ hours is because the pressure was in the process of being pumped down at this point.

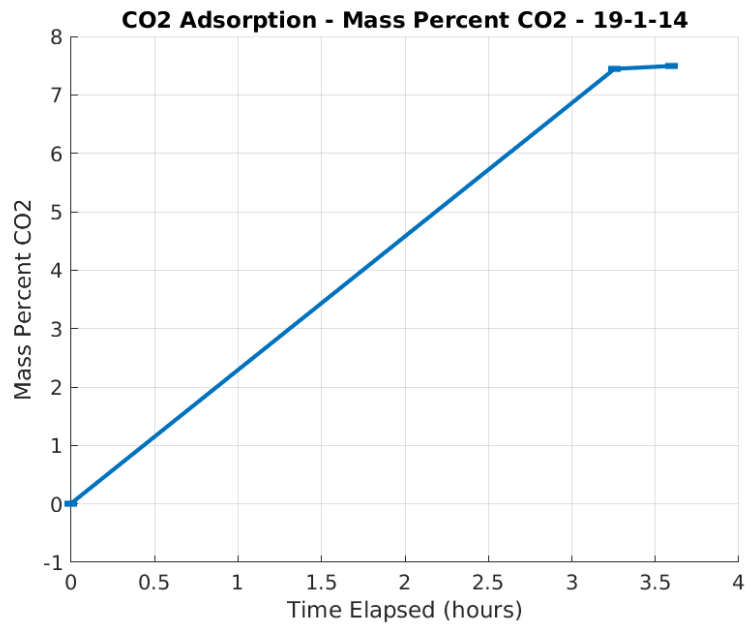


Figure 6: CO₂ sorption concentration data from January 14th

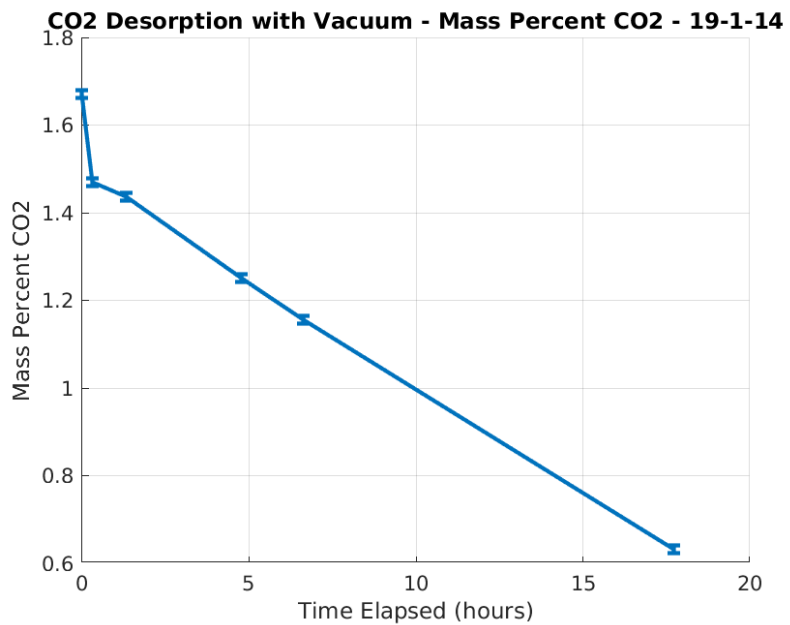


Figure 7: CO₂ desorption concentration data from January 14th

7.2 February 1st

Time Elapsed (hr)	Mass IL (g)	Pressure (mTorr)	Water Bath Temp ($^{\circ}$ C)
0.00	57.4108 \pm 0.0036	325	42
0.97	57.2654 \pm 0.0036	630	72
2.37	57.1656 \pm 0.0036	520	80
3.38	57.1069 \pm 0.0036	—	81
4.53	57.0430 \pm 0.0036	435	80
5.43	57.0112 \pm 0.0036	435	78

Table 6: Drying data from February 1st. The missing pressure data point at $t = 3.83$ hours is due to a procedural error

Time Elapsed (hr)	Mass IL (g)	CO ₂ Conc (wt. percent)
0.00	17.5165 \pm 0.0025	0.0000 \pm 0.0205
0.95	18.3063 \pm 0.0025	4.3144 \pm 0.0196
1.88	18.8101 \pm 0.0025	6.8772 \pm 0.0191
2.67	18.9707 \pm 0.0025	7.6655 \pm 0.0189
2.85	18.9761 \pm 0.0025	7.6918 \pm 0.0189

Table 7: Sorption data from February 1st

Time Elapsed (hours)	IL Mass (g)	CO ₂ Conc (wt. percent)
0.00	50.1567 \pm 0.0036	1.6692 \pm 0.0108
0.48	50.0734 \pm 0.0036	1.5056 \pm 0.0109
1.23	49.9859 \pm 0.0036	1.3332 \pm 0.0109
1.78	49.9281 \pm 0.0036	1.2190 \pm 0.0109
2.77	49.8318 \pm 0.0036	1.0281 \pm 0.0109
3.28	49.7872 \pm 0.0036	0.9394 \pm 0.0109
3.68	49.7550 \pm 0.0036	0.8753 \pm 0.0110
4.12	49.7255 \pm 0.0036	0.8165 \pm 0.0110

Table 8: Desorption data from February 1st

Time Elapsed (hours)	Pressure (mTorr)	Water Bath Temp ($^{\circ}\text{C}$)
0.00	520	76
0.48	550	84
1.23	530	82
1.78	510	84
2.77	530	81
3.28	490	81
3.68	500	76
4.12	480	78

Table 9: Pressures and Temperatures during desorption, from February 1st

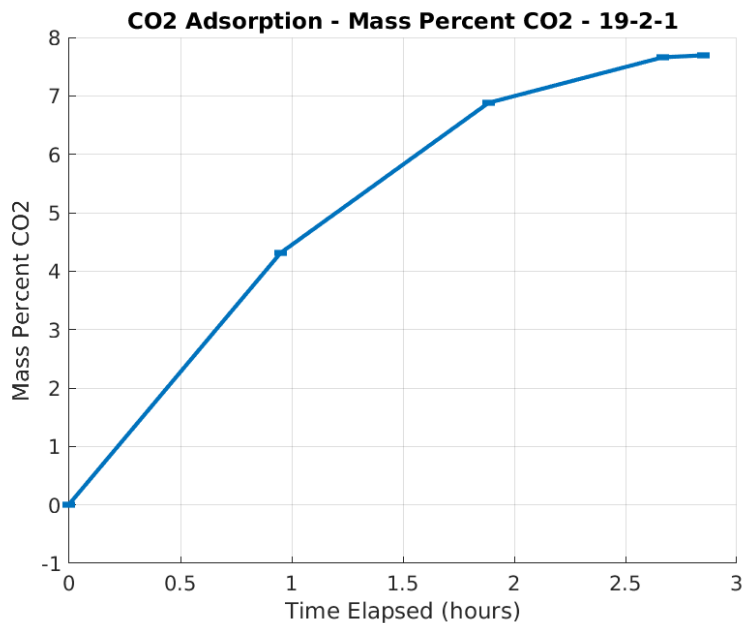


Figure 8: CO₂ sorption concentration data from February 1st

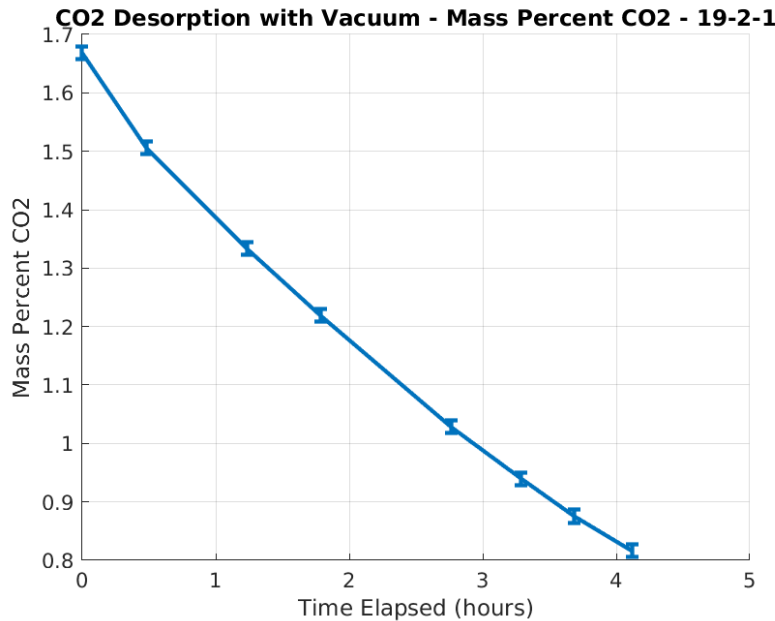


Figure 9: CO₂ desorption concentration data from February 1st

7.3 February 9th

Time Elapsed (hr)	Mass IL (g)	Pressure (mTorr)	Water Bath Temp (°C)
0.00	63.1969 ± 0.0036	600	70
1.03	62.9742 ± 0.0036	670	88
2.18	62.9207 ± 0.0036	530	80
2.90	62.8875 ± 0.0036	500	80
4.02	62.8393 ± 0.0036	530	82

Table 10: Drying data from February 9th

Time Elapsed (hr)	Mass IL (g)	CO ₂ Conc (wt. percent)
0.00	20.3852 ± 0.0025	0.0000 ± 0.0176
0.88	20.9773 ± 0.0025	2.8226 ± 0.0171
1.63	21.3657 ± 0.0025	4.5891 ± 0.0168
2.22	21.6241 ± 0.0025	5.7293 ± 0.0166
2.87	21.8227 ± 0.0025	6.5872 ± 0.0164

Table 11: Sorption data from February 9th

Time Elapsed (hours)	IL Mass (g)	CO ₂ Conc (wt. percent)
0.00	54.7207 ± 0.0036	1.6107 ± 0.0100
0.28	54.6706 ± 0.0036	1.5206 ± 0.0100
0.82	54.6520 ± 0.0036	1.4870 ± 0.0100
1.53	54.6268 ± 0.0036	1.4416 ± 0.0101
2.53	54.5935 ± 0.0036	1.3815 ± 0.0101
3.77	54.5529 ± 0.0036	1.3081 ± 0.0101

Table 12: Desorption data from February 9th

Time Elapsed (hours)	Pressure (mTorr)	Water Bath Temp (°C)
0.00	630	60
0.28	—	62
0.82	340	58
1.53	345	56
2.53	455	62
3.77	385	62

Table 13: Pressures and Temperatures during desorption, from February 9th. The missing data point at $t = 0.28$ hours is due to a procedural error.

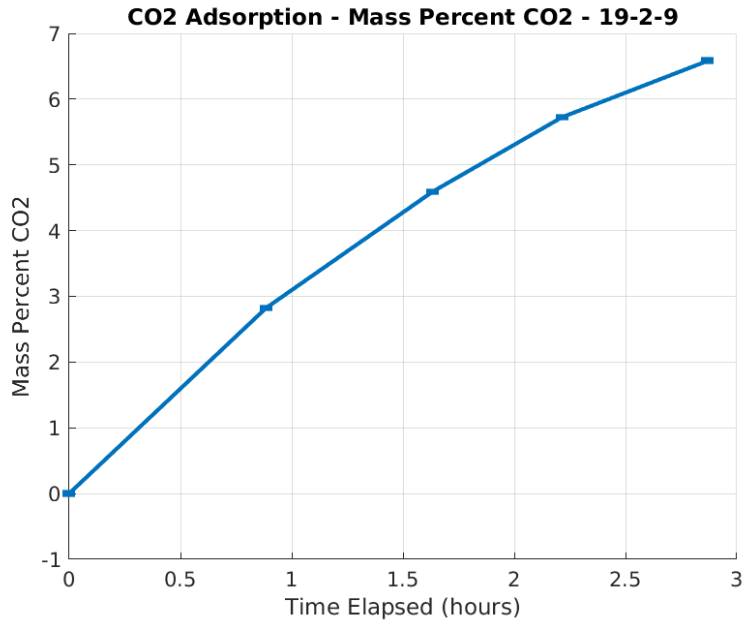


Figure 10: CO₂ sorption concentration data from February 9th

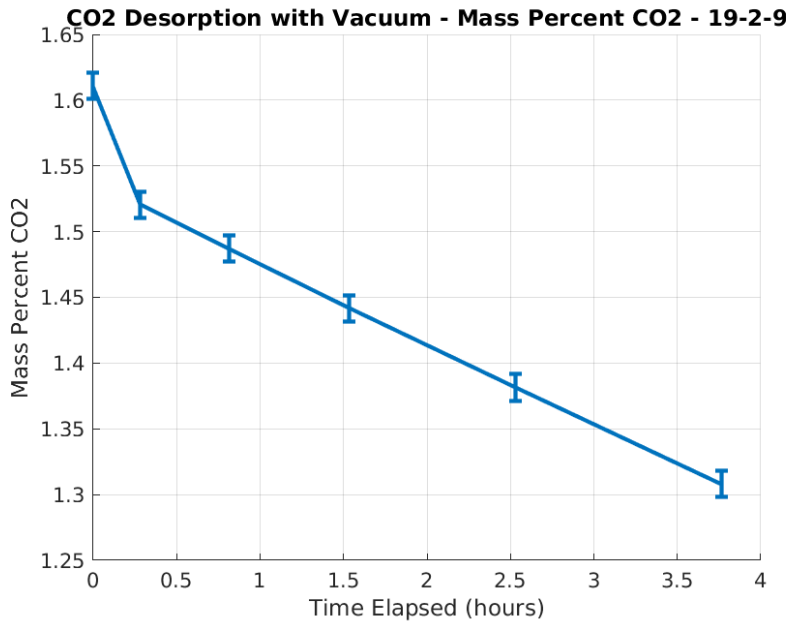


Figure 11: CO₂ desorption concentration data from February 9th

7.4 February 16th

Time Elapsed (hr)	Mass IL (g)	Water Bath Temp (°C)	Pressure (mTorr)
0.00	47.1047 ± 0.0036	67	1350
0.92	46.9944 ± 0.0036	80	445
1.50	46.9494 ± 0.0036	70	450

Table 14: Drying data from February 16th

Time Elapsed (hr)	Mass IL (g)	CO ₂ Conc (wt. percent)
0.00	13.0861 ± 0.0025	0.0000 ± 0.0274
0.83	13.4545 ± 0.0025	2.7381 ± 0.0266
2.18	13.8352 ± 0.0025	5.4145 ± 0.0259
3.02	13.9347 ± 0.0025	6.0898 ± 0.0257
3.35	13.9601 ± 0.0025	6.2607 ± 0.0257

Table 15: Sorption data from February 16th

Time Elapsed (hours)	IL Mass (g)	CO ₂ Conc (wt. percent)
0.00	45.7986 ± 0.0036	1.6880 ± 0.0130
0.53	45.6817 ± 0.0036	1.4365 ± 0.0130
0.95	45.6494 ± 0.0036	1.3667 ± 0.0130
2.05	45.5773 ± 0.0036	1.2107 ± 0.0131
3.03	45.5135 ± 0.0036	1.0722 ± 0.0131
4.00	45.4543 ± 0.0036	0.9434 ± 0.0131
4.95	45.4014 ± 0.0036	0.8280 ± 0.0131

Table 16: Desorption data from February 16th

Time Elapsed (hours)	Pressure (mTorr)	Water Bath Temp (°C)
0.00	—	66
0.53	475	67
0.95	380	66
2.05	395	69
3.03	410	70
4.00	390	69
4.95	385	70

Table 17: Pressures and Temperatures during desorption, from February 16th. The missing data point at $t = 0$ hours is because the pressure was being pumped down at this point.

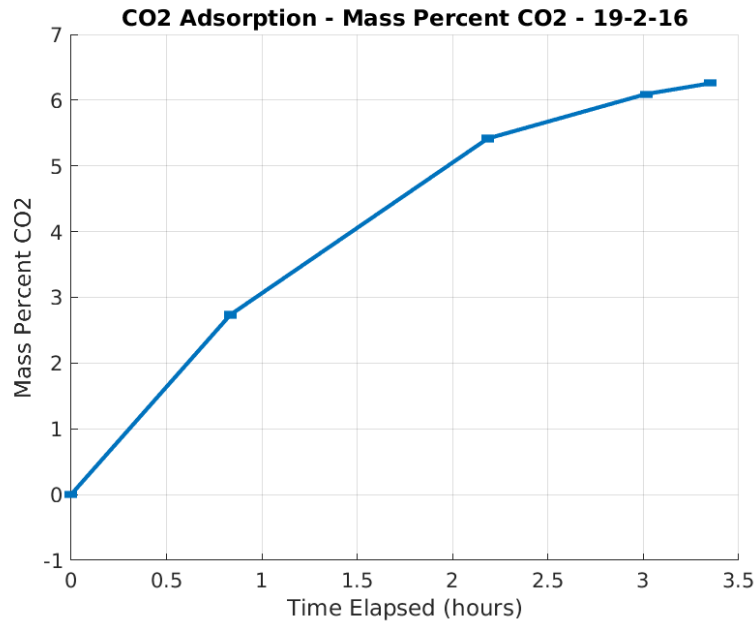


Figure 12: CO₂ sorption concentration data from February 16th

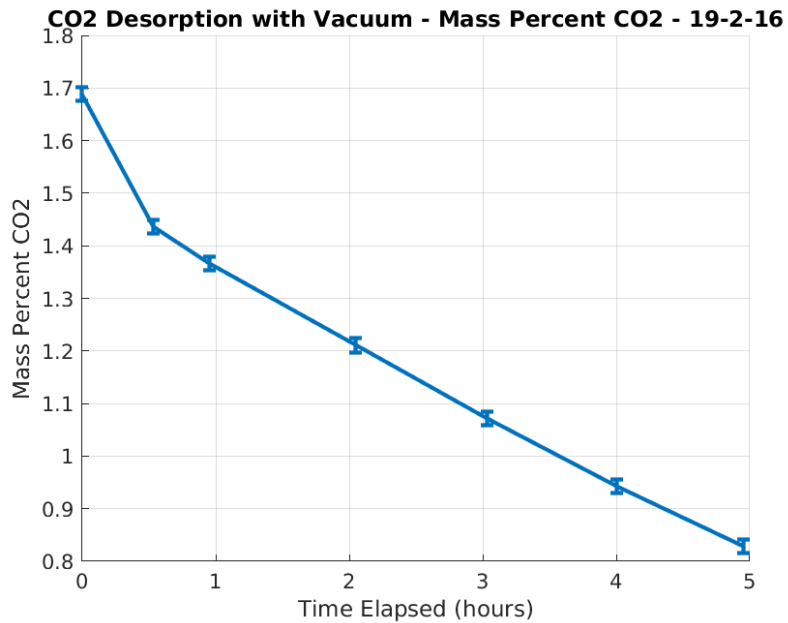


Figure 13: CO₂ desorption concentration data from February 16th

7.5 March 1st

Time Elapsed (hr)	Mass IL (g)	Temperature ($^{\circ}C$)	Pressure (mTorr)
0.00	73.0546 \pm 0.0012	51	470
0.50	72.9476 \pm 0.0012	75	520
1.05	72.9184 \pm 0.0012	77	500
1.83	72.8860 \pm 0.0011	76	475
2.83	72.8405 \pm 0.0012	77	480
3.48	72.8105 \pm 0.0012	77	490

Table 18: Drying data from March 1st

Time Elapsed (hr)	Mass IL (g)	CO ₂ Conc (wt. percent)
0.00	25.9640 \pm 0.0025	0.0000 \pm 0.0138
1.43	27.4099 \pm 0.0022	5.2753 \pm 0.0121
1.97	27.7035 \pm 0.0025	6.2790 \pm 0.0129
2.57	27.9473 \pm 0.0022	7.0966 \pm 0.0119

Table 19: Sorption data from March 1st

Time Elapsed (hours)	IL Mass (g)	CO ₂ Conc (wt. percent)
0.00	61.3884 \pm 0.0018	1.7464 \pm 0.0051
0.22	61.3396 \pm 0.0018	1.6682 \pm 0.0051
0.67	61.3073 \pm 0.0012	1.6163 \pm 0.0046
1.53	61.2531 \pm 0.0012	1.5293 \pm 0.0046
2.60	61.1910 \pm 0.0018	1.4294 \pm 0.0051
3.48	61.1360 \pm 0.0018	1.3407 \pm 0.0051
4.43	61.0784 \pm 0.0018	1.2477 \pm 0.0051
5.52	61.0180 \pm 0.0018	1.1499 \pm 0.0051
5.95	60.9921 \pm 0.0018	1.1080 \pm 0.0051

Table 20: Desorption data from March 1st

Time Elapsed (hours)	Pressure (mTorr)	Water Bath Temp ($^{\circ}\text{C}$)
0.00	—	69
0.22	540	70
0.67	550	71
1.53	510	71
2.60	510	71
3.48	510	71
4.43	540	71
5.52	540	72
5.95	520	72

Table 21: Pressures and Temperatures during desorption, from March 1st. The missing data point at $t = 0$ hours is because the pressure in the side arm flask was not stable at this time.

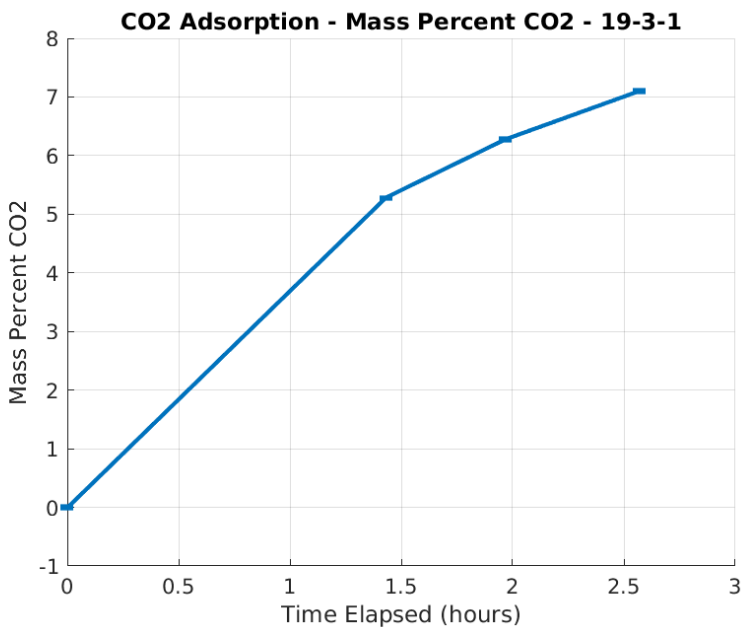


Figure 14: CO₂ sorption concentration data from March 1st

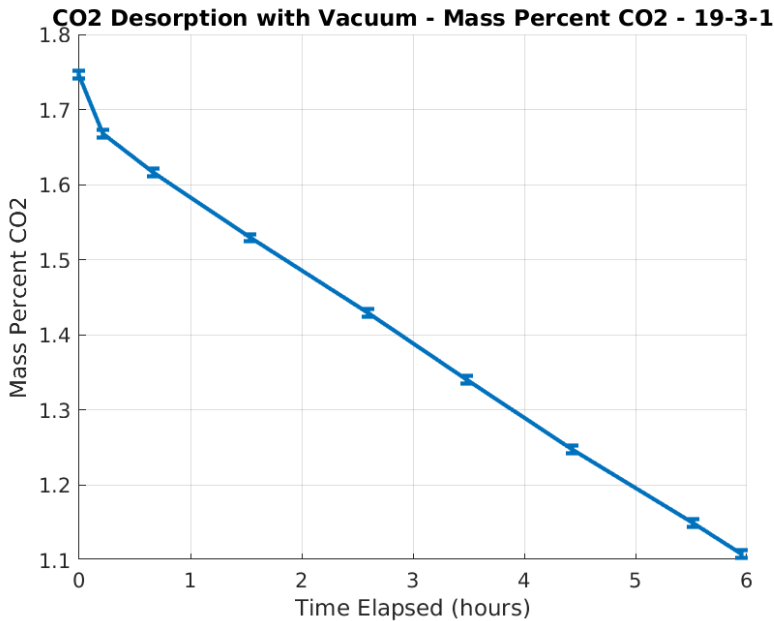


Figure 15: CO₂ desorption concentration data from March 1st

7.6 March 16th

Time Elapsed (hr)	Mass IL (g)	Water Bath Temp (°C)
0.00	55.5430 ± 0.0008	21
0.42	55.5717 ± 0.0008	21
1.25	55.5739 ± 0.0008	24
2.53	55.5586 ± 0.0008	26
3.52	55.5513 ± 0.0008	27
4.48	55.5473 ± 0.0008	26
4.85	55.5218 ± 0.0008	26

Table 22: Drying data from March 16th. Argon flow was kept between 90 and 96 scc/min.

Time Elapsed (hr)	Mass IL (g)	CO ₂ Conc (wt. percent)
0.00	19.9230 ± 0.0018	0.0000 ± 0.0117
0.60	20.3628 ± 0.0009	2.1597 ± 0.0085
1.92	21.1028 ± 0.0009	5.5906 ± 0.0082
2.67	21.2842 ± 0.0009	6.3951 ± 0.0080
3.23	21.3701 ± 0.0009	6.7718 ± 0.0081

Table 23: Sorption data from March 16th

Time Elapsed (hours)	IL Mass (g)	CO ₂ Conc (wt. percent)
0.00	46.6177 ± 0.0008	1.6551 ± 0.0032
0.72	46.6284 ± 0.0008	1.6778 ± 0.0032
1.37	46.6156 ± 0.0008	1.6508 ± 0.0032
1.83	46.6156 ± 0.0008	1.6508 ± 0.0032
2.38	46.6057 ± 0.0008	1.6298 ± 0.0032
2.87	46.5944 ± 0.0008	1.6060 ± 0.0032
3.17	46.5881 ± 0.0008	1.5927 ± 0.0032
3.43	46.5548 ± 0.0008	1.5222 ± 0.0032

Table 24: Desorption data from March 16th

Time Elapsed (hours)	Water Bath Temp (°C)
0.00	19
0.72	19
1.37	19
1.83	19
2.38	19
2.87	19
3.17	19
3.43	19

Table 25: Temperatures during desorption, from March 16th. Instead of reduced pressure, Argon was bubbled through the IL at between 90 and 96 *scc/min* in this experiment.

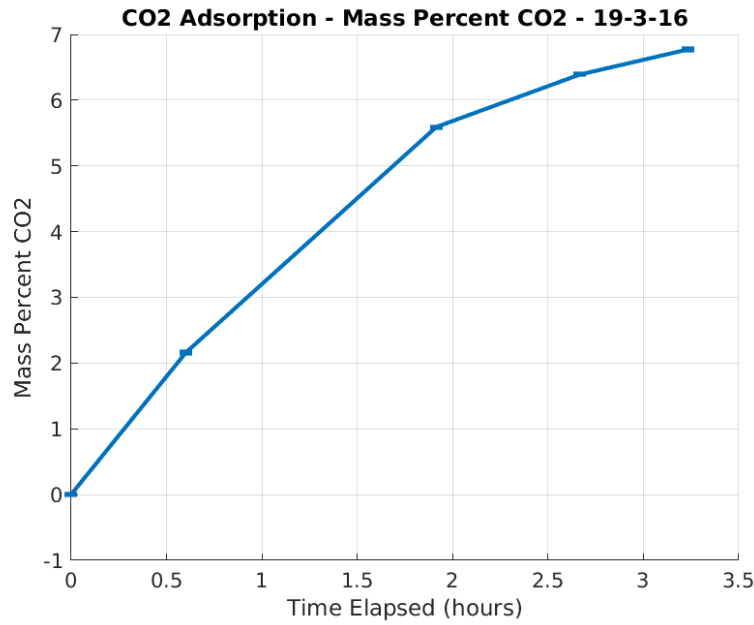


Figure 16: CO₂ sorption concentration data from March 16th

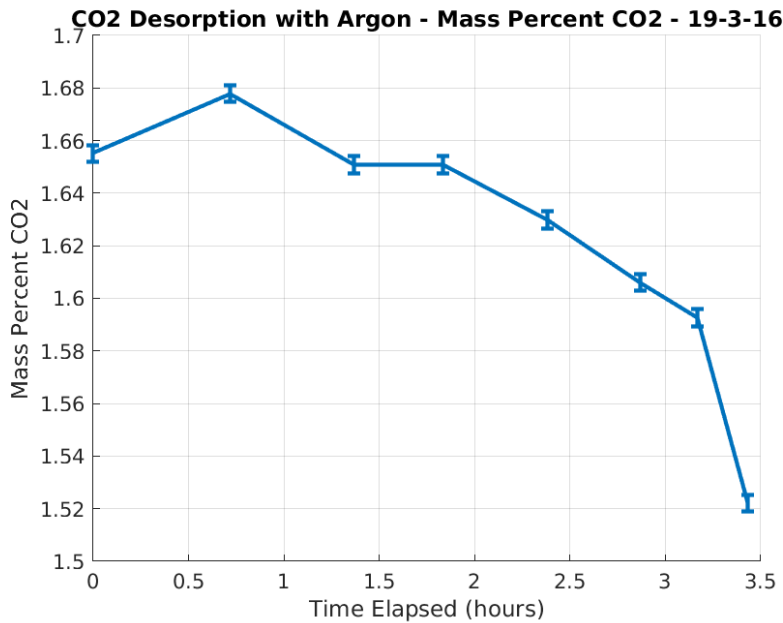


Figure 17: CO₂ desorption concentration data from March 16th

7.7 April 6th

Time Elapsed (hr)	Mass IL (g)	Water Bath Temp ($^{\circ}$ C)	Argon Flow (scc/min)
0.00	56.1569 \pm 0.0011	23	95.1
1.05	53.3950 \pm 0.0011	66	93.6
1.83	53.2106 \pm 0.0011	66	94.7
2.27	53.1327 \pm 0.0011	68	92.8
3.23	52.9612 \pm 0.0011	66	92.3
4.03	52.8595 \pm 0.0011	66	92.0
4.42	52.8312 \pm 0.0018	66	91.8

Table 26: Drying data from March April 6th.

Time Elapsed (hr)	Mass IL (g)	CO ₂ Conc (wt. percent)
0.00	16.2614 \pm 0.0008	0.0000 \pm 0.0067
0.60	16.7198 \pm 0.0008	2.7417 \pm 0.0065
1.50	17.0797 \pm 0.0008	4.7909 \pm 0.0064
2.27	17.2589 \pm 0.0008	5.7796 \pm 0.0063
2.93	17.3360 \pm 0.0008	6.1988 \pm 0.0063

Table 27: Sorption data from April 6th

Time Elapsed (hours)	IL Mass (g)	CO ₂ Conc (wt. percent)
0.00	53.6651 \pm 0.0011	1.6761 \pm 0.0033
1.05	53.3950 \pm 0.0011	1.1789 \pm 0.0034
1.83	53.2105 \pm 0.0011	0.8363 \pm 0.0033
2.27	53.1327 \pm 0.0011	0.6910 \pm 0.0034
3.23	52.9612 \pm 0.0011	0.3694 \pm 0.0034
4.03	52.8595 \pm 0.0011	0.1778 \pm 0.0034
4.42	52.8312 \pm 0.0018	0.1243 \pm 0.0043

Table 28: Desorption data from April 6th

Time Elapsed (hours)	Water Bath Temp ($^{\circ}$ C)	Argon Flow Rate (scc/min)
0.00	23	95.1
1.05	66	93.6
1.83	66	94.7
2.27	67	92.8
3.23	65	92.3
4.03	65	91.9
4.42	65	91.8

Table 29: Temperatures and flow rates during desorption, from April 6th.

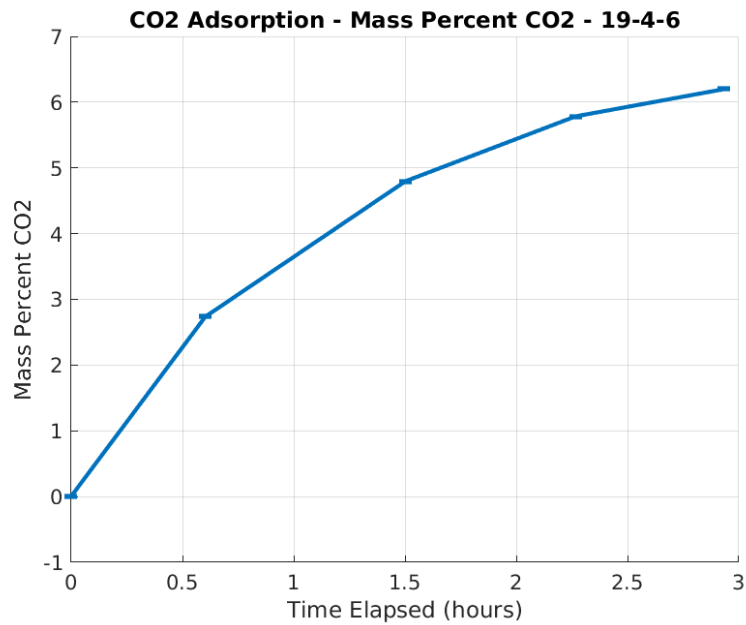


Figure 18: CO₂ sorption concentration data from April 6th

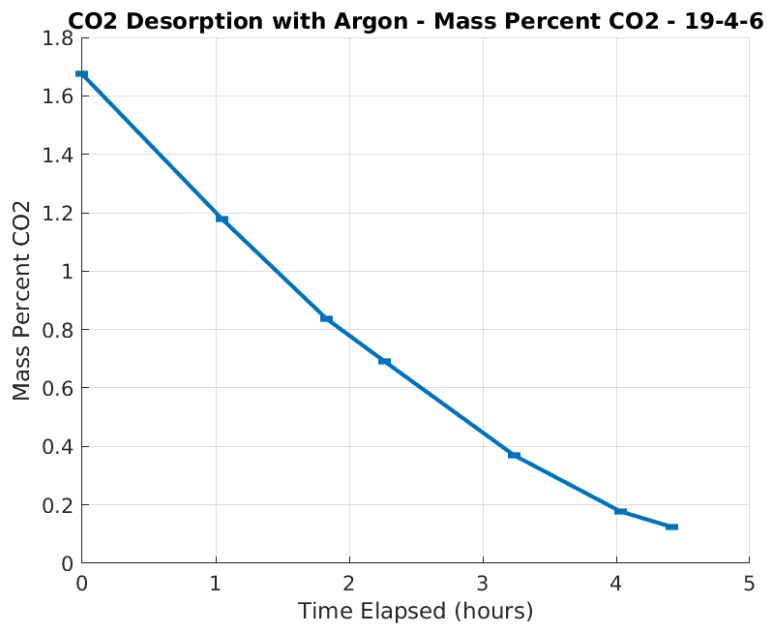


Figure 19: CO₂ desorption concentration data from April 6th

7.8 April 13th

Time Elapsed (hr)	Mass IL (g)	Water Bath Temp ($^{\circ}C$)	Argon Flow (scc/min)
0.00	51.4958 ± 0.0009	76	94.0
1.02	51.3108 ± 0.0009	77	90.7
3.00	51.0738 ± 0.0009	75	91.6
6.33	50.9185 ± 0.0008	76	90.0

Table 30: Drying data from April 13th.

Time Elapsed (hr)	Mass IL (g)	CO ₂ Conc (wt. percent)
0.00	15.3637 ± 0.0008	0.0000 ± 0.0069
0.92	15.9041 ± 0.0008	3.3978 ± 0.0068
1.90	16.3311 ± 0.0008	5.9234 ± 0.0065
2.58	16.4778 ± 0.0008	6.7607 ± 0.0066
3.42	16.5783 ± 0.0008	7.3263 ± 0.0064

Table 31: Sorption data from April 13th

Time Elapsed (hours)	IL Mass (g)	CO ₂ Conc (wt. percent)
0.00	45.5346 ± 0.0009	1.6748 ± 0.0033
0.98	45.4361 ± 0.0009	1.4617 ± 0.0032
2.07	45.2931 ± 0.0009	1.1507 ± 0.0032
2.88	45.2057 ± 0.0009	0.9595 ± 0.0032
4.07	45.1097 ± 0.0008	0.7487 ± 0.0032
4.37	45.0873 ± 0.0008	0.6993 ± 0.0032

Table 32: Desorption data from April 13th

Time Elapsed (hours)	Water Bath Temp ($^{\circ}C$)	Argon Flow Rate (scc/min)
0.00	55	93.4
0.98	63	91.7
2.07	67	91.5
2.88	66	91.6
4.07	66	91.5
4.37	68	91.5

Table 33: Temperatures and flow rates during desorption, from April 13th.

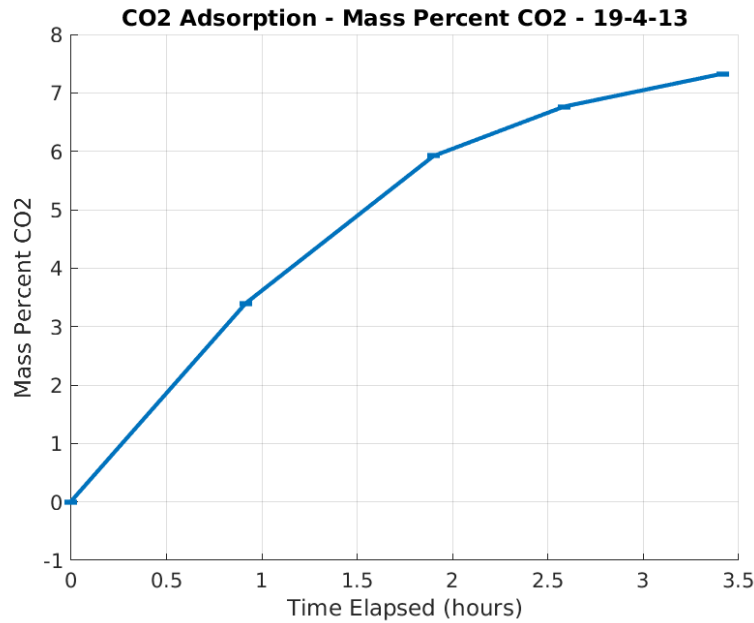


Figure 20: CO₂ sorption concentration data from April 13th

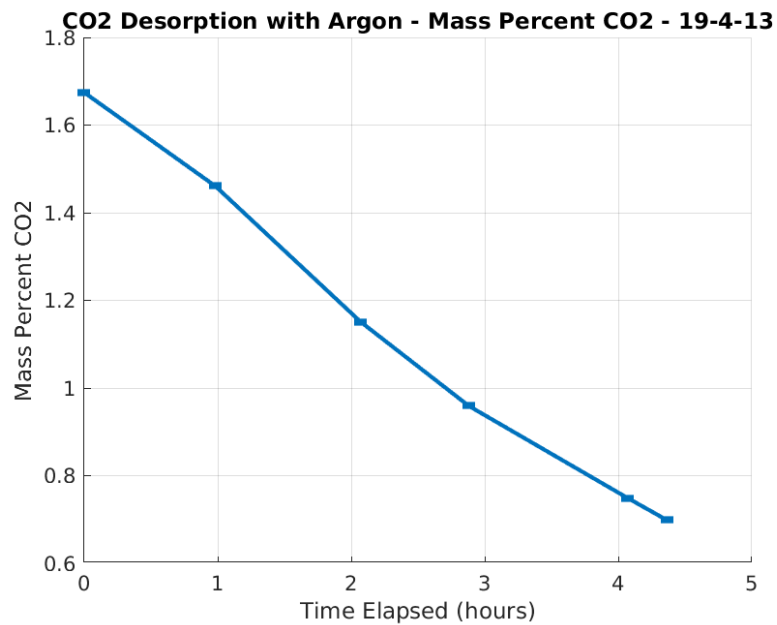


Figure 21: CO₂ desorption concentration data from April 13th

7.9 April 27th

Time Elapsed (hr)	Mass IL (g)	Water Bath Temp ($^{\circ}C$)	Argon Flow (scc/min)
0.00	49.1284 \pm 0.0017	57	95.2
0.98	48.9986 \pm 0.0017	76	91.0
2.75	48.8291 \pm 0.0017	77	88.7
4.48	48.7190 \pm 0.0017	76	94.7
6.25	48.6512 \pm 0.0017	74	93.8

Table 34: Drying data from April 27th.

Time Elapsed (hr)	Mass IL (g)	CO ₂ Conc (wt. percent)
0.00	13.0318 \pm 0.0008	0.0000 \pm 0.0083
2.07	13.8907 \pm 0.0008	6.1831 \pm 0.0081
2.47	13.9710 \pm 0.0008	6.7224 \pm 0.0080
3.07	14.0454 \pm 0.0008	7.2165 \pm 0.0080
3.38	14.0722 \pm 0.0008	7.3932 \pm 0.0080

Table 35: Sorption data from April 27th

Time Elapsed (hours)	IL Mass (g)	CO ₂ Conc (wt. percent)
0.00	45.4493 \pm 0.0017	1.6703 \pm 0.0055
1.30	45.3096 \pm 0.0017	1.3672 \pm 0.0055
2.65	45.1637 \pm 0.0017	1.0485 \pm 0.0055
3.53	45.0868 \pm 0.0017	0.8798 \pm 0.0055
4.52	45.0266 \pm 0.0017	0.7472 \pm 0.0056

Table 36: Desorption data from April 27th

Time Elapsed (hours)	Water Bath Temp ($^{\circ}C$)	Argon Flow Rate (scc/min)
0.00	50	94.9
1.30	66	93.0
2.65	66	91.9
3.53	65	91.5
4.52	65	91.6

Table 37: Temperatures and flow rates during desorption, from April 27th.

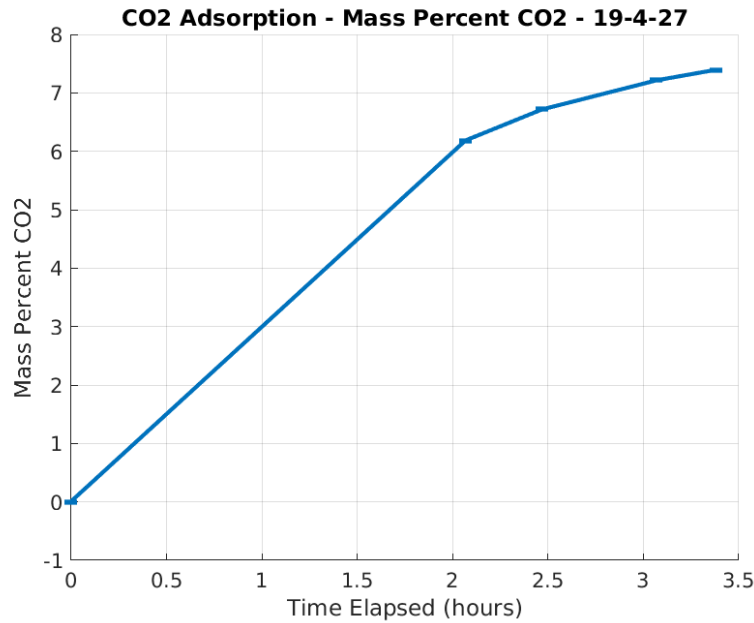


Figure 22: CO₂ sorption concentration data from April 27th

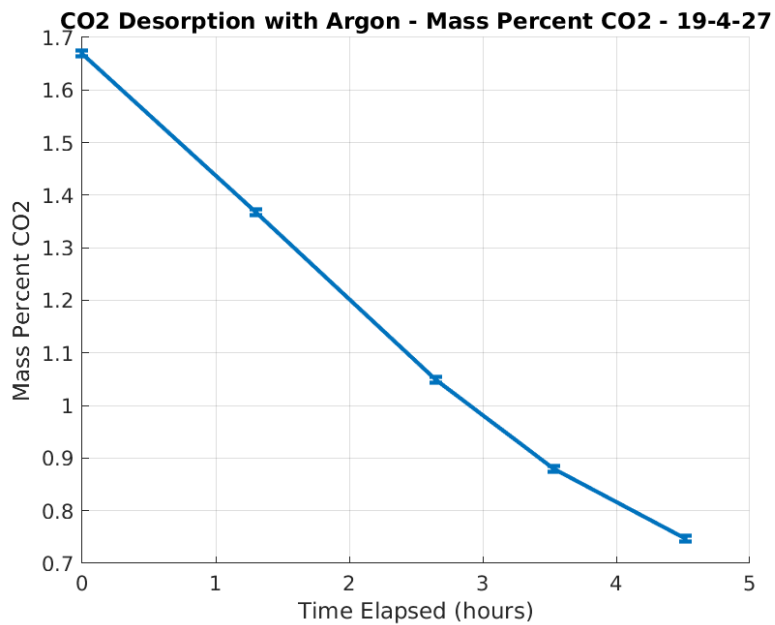


Figure 23: CO₂ desorption concentration data from April 27th

References

- [1] Cabin atmosphere revitalization through ionic liquids (caril) - final documentation. May 9, 2017.
- [2] Molly Anderson, Michael Ewert, and John Keener. *Life Support Baseline Values and Assumptions*. National Aeronautics and Space Administration, 2018.
- [3] Brett Shaffer. Regenerability of a room temperature ionic liquid used in carbon dioxide scrubbing. August 11, 2017.
- [4] Stephen F. Yates, Alexander Bershtsky, Ted Bonk, Phoebe Henson, and Allen MacKnight. Direct liquid contact – next generation approach to combined co₂ recovery and humidity control for extended missions. In *AIAA SPACE*, 2016.